

Clinical application of diffusion-weighted imaging and dynamic contrast-enhanced MRI in assessing the clinical curative effect of early ankylosing spondylitis

Zhaojuan Shi, MS^{a,b}, Jiankui Han, MD^{a,*}, Jian Qin, MS^b, Yue Zhang, MS^b

Abstract

The study aimed to demonstrate the clinical application value of diffusion-weighted imaging (DWI) and dynamic contrast-enhanced magnetic resonance imaging (DCE-MRI) in assessing a clinical curative effect of early ankylosing spondylitis (AS).

Forty-eight patients with early AS who were already treated combinations by traditional Chinese and Western medicine were involved in this study. All subjects underwent the conventional MRI, DWI, and DCE-MRI scanning of bilateral sacroiliac joints before and after treatment. The relevant data, such as the mean apparent diffusion coefficient (ADC) value, time-intensity curve of subarticular surface bone marrow, and the relationship between ADC value and enhancement factor (Fenh), enhancement slope (Senh), and time to peak (TTP), were obtained.

1. The mean ADC value of the subarticular surface bone marrow of patients and after clinical treatment was $(5.05 \pm 1.10) \times 10^{-4}$ and $(4.34 \pm 0.55) \times 10^{-4} \text{ mm}^2/\text{s}$ in ilium and $(4.63 \pm 0.79) \times 10^{-4}$ and $(3.96 \pm 0.23) \times 10^{-4} \text{ mm}^2/\text{s}$ in sacrum, respectively. 2. In the DCE-MRI follow-up treatment imaging of 48 patients with AS (192 parts), the TIC curve type recorded was as follows: 43.75% (84/192) of type II, 56.25% (108/192) of type III, and type I curve was not seen. The number of type II curve was significantly reduced for pre treatment group (84 cases) compared with that post treatment group (124 cases). The Fenh, Senh, and TTP values were respective $(113.38 \pm 44.71)\%$, $(60.94 \pm 38.56)\%$ min, $(129.52 \pm 42.66)\text{s}$ in ilium and $(83.03 \pm 20.39)\%$, $(44.91 \pm 15.19)\%$ min, $(123.44 \pm 28.50)\text{s}$ in sacrum before clinical treatment. After the treatment, the Fenh, Senh, and TTP values were respective $(75.90 \pm 17.97)\%$, $(33.96 \pm 11.36)\%$ min, $(138.67 \pm 26.60)\text{s}$ in ilium and $(73.28 \pm 15.67)\%$, $(31.92 \pm 8.15)\%$ min, $(140.19 \pm 19.88)\text{s}$ in sacrum. The Fenh, Senh, and TTP values of semiquantitative indexes before and after clinical treatment were significantly different.

DWI and DCE-MRI sequences can help evaluate the degree of active changes in AS inflammation and treatment effect in patients with early AS, and provide reliable imaging evidence.

Abbreviations: ADC = apparent diffusion coefficient, AS = ankylosing spondylitis, CRP = C-creative protein, CT = computed tomography, DCE-MRI = dynamic contrast-enhanced MRI, DWI = diffusion weighted imaging, ESR = erythrocyte sedimentation rate, Fenh = enhancement factor, HLA-B27 = human leukocyte antigen-B27, MRI = magnetic resonance imaging, ROI = regions of interest, Senh = enhancement slope, SI = signal intensity, SI_0 = initial signal intensity, SI_{max} = maximum signal strength, STIR = short time inversion recovery, T1W FSE = T1-weighted fast spin echo, T2W FSE = T2-weighted fast spin echo, TIC = time-signal intensity curve, TTP = time to peak.

Keywords: ankylosing spondylitis, diffusion-weighted imaging, dynamic contrast-enhanced, magnetic resonance, therapeutic effect

Editor: Ilke Coskun Benlidayi.

ZS and JH authors contributed equally to this work.

All procedures performed in studies involving human participants were in accordance with the ethical standards of the institutional and/or national research committee and with the 1964 Helsinki declaration and its later amendments or comparable ethical standards.

The authors declare that they have no conflict of interest.

^a Department of Nuclear Medicine, Qilu Hospital, Shandong University, Jinan, ^b Department of Diagnostic Radiology, Affiliated Hospital of Taishan Medical University, Taian, Shandong, China.

* Correspondence: Jiankui Han, Department of Nuclear Medicine, Qilu Hospital, Shandong University, 107 Wenhua West Road, Jinan, Shandong 250012, China (e-mail: jkhan@sdu.edu.cnhanjiankui2006@163.com).

Copyright © 2019 the Author(s). Published by Wolters Kluwer Health, Inc.

This is an open access article distributed under the terms of the Creative Commons Attribution-Non Commercial-No Derivatives License 4.0 (CCBY-NC-ND), where it is permissible to download and share the work provided it is properly cited. The work cannot be changed in any way or used commercially without permission from the journal.

Medicine (2019) 98:20(e15227)

Received: 15 January 2018 / Received in final form: 28 February 2019 / Accepted: 20 March 2019

<http://dx.doi.org/10.1097/MD.00000000000015227>

1. Introduction

Ankylosing spondylitis (AS) is a chronic inflammatory disease affecting mainly young adults and belongs to the group of multiple seronegative spondyloarthropathy. It usually starts from the sacroiliac joint with an upstream trend involving the axis joints and other auxiliary structures, characterized by extensive fibrosis, osteoankylosis, and lesions in multiple systems in the advanced stage. Delayed treatment results in multiple dysfunction and disability, seriously affecting the quality of life of patients.^[1] Therefore, diagnosis and clinical intervention at the early stage of AS is important. The present study included patients with early AS who have been diagnosed and remedied with Chinese traditional and Western medicine (such as Radix Paeoniae Alba, *Tripterygium wilfordii*,^[2] sulfasalazine,^[3] non-steroidal anti-inflammatory drugs,^[4] and so on). The changes in water molecular diffusion in subsacroiliac surface bone marrow before and after treatment were analyzed using diffusion-weighted imaging (DWI) and dynamic contrast-enhanced magnetic resonance imaging (DCE-MRI) scans. This was done to identify treatment efficacy and changes in radiographs in early AS, which may offer reliable imaging evidence and new ideas for clinical treatment.

2. Materials and methods

2.1. Materials

The present study was approved by the institutional review board. The patients had no contraindications of MRI and gave written informed consent.

Under the revised “New York standards”, combined with clinical signs and symptoms and laboratory test results, retrospectively collected early clinical activity of 48 patients with AS during the 2014 to 2016 in my hospital. All cases were evaluated by MRI before and after about 6 months treatment with combination of traditional Chinese and Western medicine, which judged the curative effect according to signal changes and related datum. There were pre-treatment patients as the control groups and post-treatment patients as the case groups.

A total of 48 patients (38 men and 10 women, age range 14–42 years) with early AS were included in this study. Patients were with 0.5 to 6 years of disease duration and had been treated for more than half a year with a combination of Chinese and Western medicine. Of these patients, 43 (89.5%) had low back pain (27 with bilateral pain and 16 with unilateral pain), 23 (47.9%) had morning stiffness, and 7 (14.6%) had extra-axis joint symptoms. Also, 44 (91.7%) patients were positive for human leukocyte antigen-B27 (HLA-B27), 30 (62.5%) had increased blood sedimentation (erythrocyte sedimentation rate [ESR]), and 39

(81.2%) had increased C-reative protein (CRP) by different degrees in laboratory examination.

The criteria for the selection of patients as follows:

1. According to New York revised diagnostic criteria for AS in 1984, no abnormal findings were found on X-ray or computed tomography (CT) as Grade 0, which blurred articular surface, plaque-like decalcification, local cortical sclerosis, subchondral microcapsule degeneration, but normal articular space, was classified as Grade I-II. If the image shows obvious destruction, extensive sclerosis, serrated changes of articular surface and narrowing or rigidity of articular space of subchondral bone on X-ray or CT, which was classified as Grade III-IV. Patients with Grade 0-II by X-ray or CT findings were taken as case group and excluded Patients with Grade III-IV. All patients must have clinical symptoms and laboratory examinations to support the diagnosis of AS.
2. All patients had no contraindication of MRI. They accepted the MRI examination voluntarily and signed the informed consent. All patients received the same parameters and sequences in MRI before and after treatment.
3. All the patients were treated with the combination of Chinese and Western medicine. But, the dosage and duration of drugs were not entirely consistent because it is difficult to unify the personal specific conditions in all patients which were its shortages.

2.2. MRI

2.2.1. MRI equipment and sequences. MRI scanning was performed for all patients using a 3.0 T MR (GE Discovery MR 750, GE Medical Systems, LLC, WI) with a cardiac quadrature coil. Five MR sequences were obtained:

1. oblique coronal T1-weighted fast spin-echo sequence (T1W-FSE),
2. oblique coronal T2-weighted fast spin-echo sequence (T2W-FSE),
3. oblique coronal short time inversion recovery (STIR),
4. DWI ($b=600\text{ s/mm}^2$), and
5. DCE-MRI using volume acceleration sequence and 15 mL gadopentetate dimeglumine as a contrast agent with a 2.0 mL/s injection rate.

The direction of the scanner was parallel to the ligature between the first and second sacral vertebrae (Table 1).

2.2.2. Image analysis. The DWI original data were analyzed using the GE MRA W4.6 workstation (GE Medical Systems, LLC). First, regions of interest (ROI) were chosen, which included regions with obvious lesions in the image whose

Table 1
Imaging scanner parameters for 5 MR sequences.

| | T1W-FSE | T2W-FSE | STIR | DWI | DCE |
|--------------------------|-----------|-----------|-----------|-----------|-----------|
| TR, ms | 400 | 2400 | 2700 | 5000 | 4.3 |
| TE, ms | 10 | 110 | 110 | 50 | 3.0 |
| FOV, mm | 280 × 280 | 280 × 280 | 280 × 280 | 380 × 380 | 340 × 340 |
| Slice thickness, mm | 4 | 4 | 4 | 4 | 4 |
| Slice space, mm | 1 | 1 | 1 | 1.5 | 0 |
| Scanning number of plies | 18 | 18 | 18 | 20 | 11 |

DCE = dynamic contrast-enhanced, DWI = diffusion-weighted imaging, FOV = field of view, STIR = short T1 inversion recovery, T1W-FSE = T1-weighted fast spin-echo sequence, T2W-FSE = T2-weighted fast spin-echo sequence, TE = echo time, TR = repetition time.

location and area were consistent with the previous study. If the lesions were not obvious, 12 ROI were chosen on upper, middle, and lower areas of the subsurface bone marrow of bilateral sacrum and ilium. Subsequently, the average value of apparent diffusion coefficient (ADC) was calculated and recorded. The ROI selection should avoid the joint space, bone cortex, bone sclerosis area, blood vessels, and artifacts, and so on.

All DCE data from the group of multiple seronegative spondyloarthropathy were transferred to a postprocessing workstation for analysis. The selection of ROI was the same as DWI. However, the selected ROI were as large and included the sacral or iliac bone marrow regions when the lesions were not obvious. Following the selection of ROI, the time–signal intensity curve (TIC) was drawn automatically on the workstation, the X-axis of which was time (s) and the y-axis was the signal intensity (SI). Subsequently, the initial signal intensity (SI₀), the maximum signal strength (SI_{max}), and time to peak (TTP) were automatically exhibited on the curve. Finally, the semiquantitative index enhancement factor (Fenh) and enhancement slope (Senh) were calculated according to the following formula:

$$\text{Fenh}(\%) = (\text{SI}_{\text{max}} - \text{SI}_0) \times 100/\text{SI}_0$$

$$\text{Senh}(\% \text{min}) = (\text{SI}_{\text{max}} - \text{SI}_0) \times 100/(\text{SI}_0 \times \text{TTP})$$

2.2.3. Observation index. The MRI findings of all sequences were reviewed in a double-blind fashion by 2 experienced radiologists. Multiple MRI sequence images were comprehensively observed (T1W–FSE, T2W–FSE, STIR, DWI, and DCE), and the images were compared before and after the treatment. The changes in ADC value and TIC curve were analyzed and Fenh and Senh were calculated, which determined the changes in inflammation after the clinical treatment.

2.2.4. Statistical analysis. The statistical software SPSS 13.0 (SPSS, Chicago, IL) was used in this study.

① The values of ADC, Fenh, Senh, and TTP were expressed as mean ± standard deviation, with 95% confidence interval (95% CI). These values were used for the Wilcoxon sign-rank test.

② The scatter plots of the ADC value with Fenh value and Senh value of sacroiliac joint were drawn and analyzed the Spearman correlation analysis.

A *P* value <.05 was considered as statistically significant.

3. Results

Following medicine intake, 48 patients with symptoms had different degrees of mitigation, with one achieving a complete symptomatic relief of back pain, and normal ESR and CRP. In the relevant laboratory tests, the positive rate of HLA-B27 had no obvious change; however, ESR and CRP significantly decreased after treatment. In the AS group, before treatment, the mean ESR was 32.6 ± 26.0 mm/Hg (range 2–90 mm/Hg) and the mean serum CRP was 23.8 ± 28.5 mg/L (range 2.6–109.8 mg/L). Following treatment, the mean ESR was 16.3 ± 16.0 mm/Hg (range 2–65 mm/Hg) and the mean serum CRP was 7.2 ± 7.6 mg/L (range 0.5–36.3 mg/L).

3.1. Comparing the ADC, Fenh, Senh, and TTP values of the subarticular surface bone marrow of sacroiliac joint in the before- and after-treatment groups

Following treatment, the ADC, Fenh, Senh, and TTP values of the subarticular surface bone marrow of the sacroiliac joint were

Table 2
Index difference between before- and after-treatment groups.

| | Before treatment | After treatment | F | P |
|---|------------------|-----------------|--------|------|
| ADC value (× 10 ⁻⁴ mm ² /s) | | | | |
| Ilium | 5.05 ± 1.10 | 4.34 ± 0.55 | 31.131 | .000 |
| Sacrum | 4.63 ± 0.79 | 3.96 ± 0.23 | 63.044 | .000 |
| Fenh, % | | | | |
| Ilium | 113.38 ± 44.71 | 75.90 ± 17.97 | 29.035 | .000 |
| Sacrum | 83.03 ± 20.39 | 73.28 ± 1.67 | 6.889 | .003 |
| Senh, % min | | | | |
| Ilium | 60.94 ± 38.56 | 33.96 ± 11.36 | 21.622 | .000 |
| Sacrum | 44.91 ± 15.19 | 31.92 ± 8.15 | 27.245 | .000 |
| TTP, s | | | | |
| Ilium | 129.52 ± 42.66 | 138.67 ± 26.60 | 1.588 | .006 |
| Sacrum | 123.44 ± 28.50 | 140.19 ± 19.88 | 11.153 | .004 |

ADC=apparent diffusion coefficient, TTP=time to peak.

significantly lower than those before treatment. A significant difference was observed between the groups (*P*<.05) (Table 2).

3.2. The Spearman correlation analysis between ADC and Fenh or Senh values in different parts of bone marrow area in the case group

The correlation coefficient between ADC and Fenh values were as follows: ilium (0.744) and sacrum (0.702). The correlation coefficient between ADC and Senh values were as follows: ilium (0.738) and sacrum (0.574). All these had a highly positive correlation and were statistically significant (*P*=.000 <.05) (Table 3 and Figs. 1–4).

The Spearman’s rho correlation analysis exhibited a highly positive correlation between ADC and Fenh values in ilium (*P*=.000 <.05, *r*=0.744; Fig. 1), between ADC and Fenh values in sacrum (*P*=.000 <.05, *r*=0.702; Fig. 2), and between ADC and Senh values in ilium (*P*=.000 <.05, *r*=0.738; Fig. 3). However, a moderate positive correlation was exhibited in ADC and Fenh values in sacrum (*P*=.000 <.05, *r*=0.547; Fig. 4).

4. Discussion

The main manifestation of AS was progressive inflammation in the sacroiliac joint and spine little joints, with a possible correlation with heredity and environment but with an unclear pathogenesis.^[5]

In the clinical diagnosis and treatment process, imaging is an important method to evaluate the activity in AS and monitor for

Table 3
Correlation analysis between ADC value and Fenh and Senh values in the sacroiliac joint.

| | Correlation coefficient (r) | | P |
|--------|-----------------------------|--------------------|------|
| | ADC value (ilium) | ADC value (sacrum) | |
| Fenh | | | |
| Ilium | 0.744 | | .000 |
| Sacrum | | 0.702 | .000 |
| Senh | | | |
| Ilium | 0.738 | | .000 |
| Sacrum | | 0.574 | .000 |

ADC=apparent diffusion coefficient.

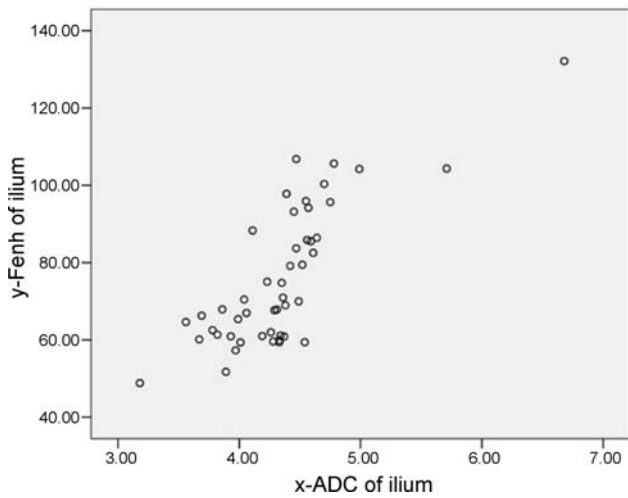


Figure 1. Scatter diagram with ADC values and Fenh values of the iliac side in the sacroiliac joint. The Spearman's rho correlation analysis exhibited a highly positive correlation between ADC and Fenh values in ilium ($P = .000 < 0.05, r = 0.744$). ADC=apparent diffusion coefficient.

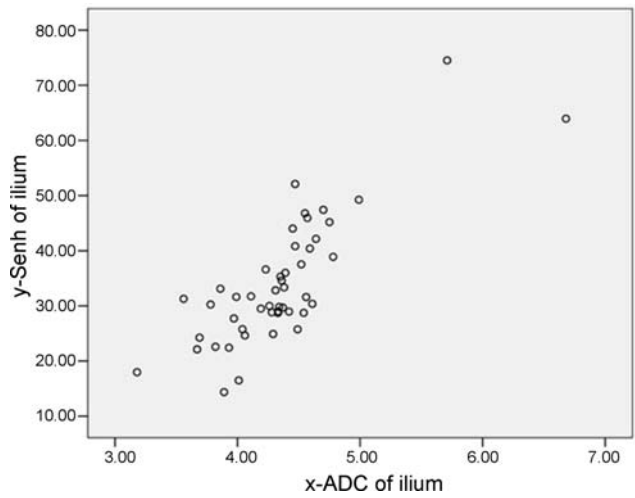


Figure 3. Scatter diagram with ADC and Senh values of the iliac side in the sacroiliac joint. The Spearman's rho correlation analysis exhibited a highly positive correlation between ADC and Senh values in ilium ($P = .000 < 0.05, r = 0.738$). ADC=apparent diffusion coefficient.

any changes. In the past, it was generally believed that X-ray film was the first method to evaluate the sacroiliac arthritis of the patients with mandatory spondylitis. However, some studies and clinical practice have found that X-ray is less sensitive to sacroiliac joint lesions, especially when there is no bone change in early AS. In addition, X-ray film can only better show the direction of the same direction of the joint surface and bone space, but not more detailed multi-angle observation of the lesion.^[6] Therefore, X-ray plain film for early diagnosis of sacroiliac joint has certain limitations, and its clinical significance is relatively low in the clinic practice.

The advantages of CT include its wide availability, speed of image acquisition, relatively low cost and multi-dimensional reconstruction. However, the main concern of CT is the risk of

exposure to ionizing radiation, especially in patients requiring continuous studies to monitor the efficacy of treatments.^[7] Comparing with X-ray, CT can not only display the whole structure of sacroiliac joint but also better observe the changes of pathological details, such as bone trabecular changes, subarticular wormlike bone destruction, articular surface roughness, bone cyst lesions, bone hyperplasia, and sclerosis and other changes in bone structure. Compared with MRI, the changes of bone marrow edema, fat deposition cannot be shown on CT, which has some limitations in evaluating the active value of sacroiliac arthritis.^[6]

MRI is a non-invasive examination with multi-parameter, multi-plane imaging, which can effectively show fat deposition and so on, articular cartilage signal changes, bone marrow

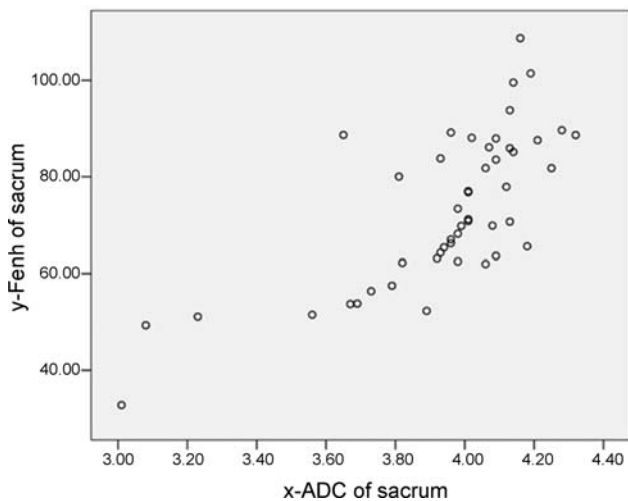


Figure 2. Scatter diagram with ADC values and Fenh values of the sacral side in the sacroiliac joint. The Spearman's rho correlation analysis exhibited a highly positive correlation between ADC and Fenh values in sacrum ($P = .000 < 0.05, r = 0.702$). ADC=apparent diffusion coefficient.

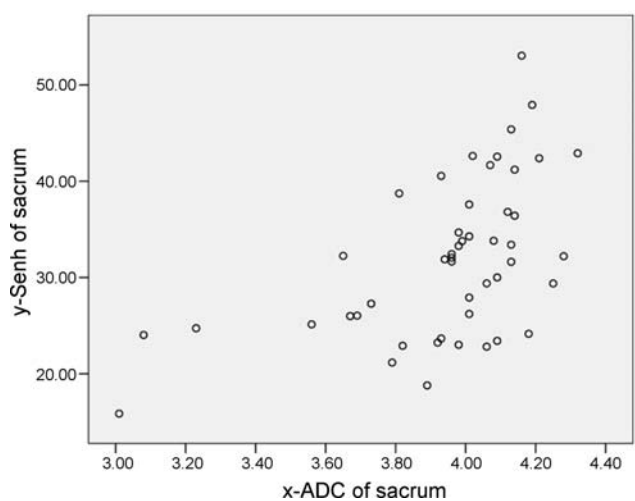


Figure 4. Scatter diagram with ADC values and Fenh values of the sacral side in the sacroiliac joint. The Spearman's rho correlation analysis exhibited a moderate positive correlation between ADC and Fenh values in sacrum ($P = .000 < 0.05, r = 0.547$). ADC=apparent diffusion coefficient.

edema. Therefore, MRI has great advantages compared with traditional radiological examination methods (X-ray, CT). In recent years, many studies have shown that MRI has unique advantages in sacroiliac joint lesions, especially in the early sensitivity to inflammation. It was reported that MRI is generally recognized as the most sensitive and specific clinical examination for diagnosing sacroiliac arthritis at the clinical radiology Symposium on sacroiliac arthritis held in Austria in 2003.^[18]

Using MRI to diagnose and evaluate active AS has been widely accepted, including different scoring systems and functional MRI methods, such as diffusion-weighted imaging (DWI) and DCE-MRI.^[9,10]

DWI and DCE-MRI may be effective methods in quantifying inflammatory changes at involved skeletal sites and useful for assessing treatment efficacy in ankylosing shown by some recent studies.^[11,11] However, the ADC value in

DWI is affected by b value, and semiquantitative parameters derived from the signal intensity–time curve in DCE-MRI could only reflect the characteristics of tissue enhancement. Quantitative permeability parameters were derived using a pharmacokinetic model through analysis of the signal intensity–time curve of the tissues.^[12] At present, some experts suggest that DWI and DCE-MRI may not only be effective methods in quantifying inflammatory changes at involved skeletal sites but also useful for assessing treatment.^[13]

In this study, we observed the change of water molecule diffusion state by measuring the ADC value, analyzed the changes of blood perfusion states by signal intensity time relation (TIC) curve, F_{enh} , $Senh$ and peak time T_{max} value, and discussed the correlation between ADC value and F_{enh} and $Senh$ values in sacroiliac joint lesions of AS before and after treatment.

4.1. Imaging features of AS in MRI routine sequences

The T1-weighted images (T1WIs) displayed the structure of the sacroiliac joint cartilage and subchondral region and provided some value in the differentiation of subchondral bone marrow fat deposition. The T2-weighted images (T2WIs) displayed joint effusion and distinguished between articular cartilage and joint effusion effectively through a large signal contrast. STIR sequences exhibited the structure and pathological changes in the sacroiliac joint and effectively identified the abnormal changes in bone marrow edema and fat deposition. The degree of inflammation of AS was analyzed mainly from articular cartilage, bone marrow edema, joint effusion, and fat deposition. An abnormal change in articular cartilage is a reliable sign of early AS, which are manifested mainly as normal signal interruption, disappearance and cartilage surface roughness, and fragmentation on the T1WIs and T2WIs. The abnormal articular cartilage signal exhibited mixed hyperintense and hypointense signal on T1WIs and irregular hyperintense signal on T2WIs. The main manifestations of bone marrow edema exhibited patchy hypointense signal on T1WIs, and hyperintense signal on T2WIs and STIR images. The joint effusion displayed low signal on T1WIs and high signal on T2WIs. The fat deposition displayed hyperintense signal on T1WIs and T2WIs and hypointense signal on STIR sequences. Asymmetric fat deposition in the bone marrow is more valuable in the diagnosis of AS.^[14]

4.2. DWI changes in early AS after treatment

Diffusion-weighted MR imaging (DWI) is the only imaging method based on the water molecular detection, in which image

contrast is due to the different random motions of water protons in different biological tissue environments. The method has proven to be an effective diagnostic tool whenever a change in the ratio of extracellular water (with low DWI signal) to intracellular water (with high DWI signal) occurs, which may be due to inflammation.^[15] Diffusion is the random thermal motion of gaseous or liquid molecules and MR imaging can detect signal changes caused by positional changes of molecules. In biological tissue, water exchange occurs between intracellular and extracellular compartments and is based on the shape of the extracellular space and tissue cellularity, which affect diffusion.^[16] DWI was obtained by application of symmetric pairs of equally weighted diffusion sensitizing gradients about the 180° refocusing pulse of spin echo T2-weighted sequence. The reduction on diffusion MR imaging can be quantified by calculating the apparent diffusion coefficient (ADC), which depends largely on the presence of barriers to diffusion within the water micro-environment.^[16]

Diffusion sensitive factor (b value) is the diffusion sensitivity coefficient of DWI. It is an index to detect the sensitivity of water molecule free diffusion. The b value is proportional to the sensitivity of water molecule movement and the change of signal and the sensitivity of water molecule movement increases with the increase of the b value. It is the product of the gyromagnetic ratio, the strength of the diffusion-sensitizing gradients, the duration of the gradient pulse and the time interval between gradient pairs.^[17–19] The choice of b value is most likely the pivotal issue of diffusion MR imaging. Diffusion-weighted imaging is typically performed with at least 2 b values to allow for the calculation of the ADC value. Previous studies reported^[20] that the structure of peri-sacroiliac joint tissue would be better reflected and the clinical observation would be better performed with a best “ b value” of 600 s/mm^2 . For patients with early AS in sacroiliac joints, incrustation of synovial lining cell layer infiltration of inflammatory cells, formation of pannus, and invasion of subarticular sclerotin resulted in bone marrow edema that was reflected in the subsacroiliac joint surface bone marrow area as a spot or patchy diffusion-restricted region (high signal area) on DWI image.

The diffusion coefficient (D) was used to measure the range of free movement of water molecules. However, ADC values were used to quantify the diffusion rate of water molecules because D is easy to be affected by many factors. In the present study, the ADC value of AS lesions increased in the bone marrow edema area. Bozgeyik^[11] believed that the presence of bone marrow edema leads to acceleration of the local water molecule movement, strengthening of the free diffusion movement, and increase in the ADC value of the diseased area.

Before clinical treatment, the mean of ADC value of the subarticular surface bone marrow of patients was $(5.05 \pm 1.10) \times 10^{-4} \text{ mm}^2/\text{s}$ in ilium and $(4.63 \pm 0.79) \times 10^{-4} \text{ mm}^2/\text{s}$ in sacrum. The mean of ADC value after the clinical intervention treatment group was $(4.34 \pm 0.55) \times 10^{-4} \text{ mm}^2/\text{s}$ in ilium and $(3.96 \pm 0.23) \times 10^{-4} \text{ mm}^2/\text{s}$ in sacrum, and both of them were significantly lower than those before treatment ($P < .05$). Therefore, these data revealed that the degree of infiltration of inflammatory cells, formation of pannus, and formation of bone marrow edema decreased after intervention treatment. Moreover, the region for restricted water diffusion became smaller in the corresponding position, and the signal of the DWI diffusion-restricted region reduced with ADC value lowered compared with that before treatment (Fig. 5). However, the ADC value was still slightly

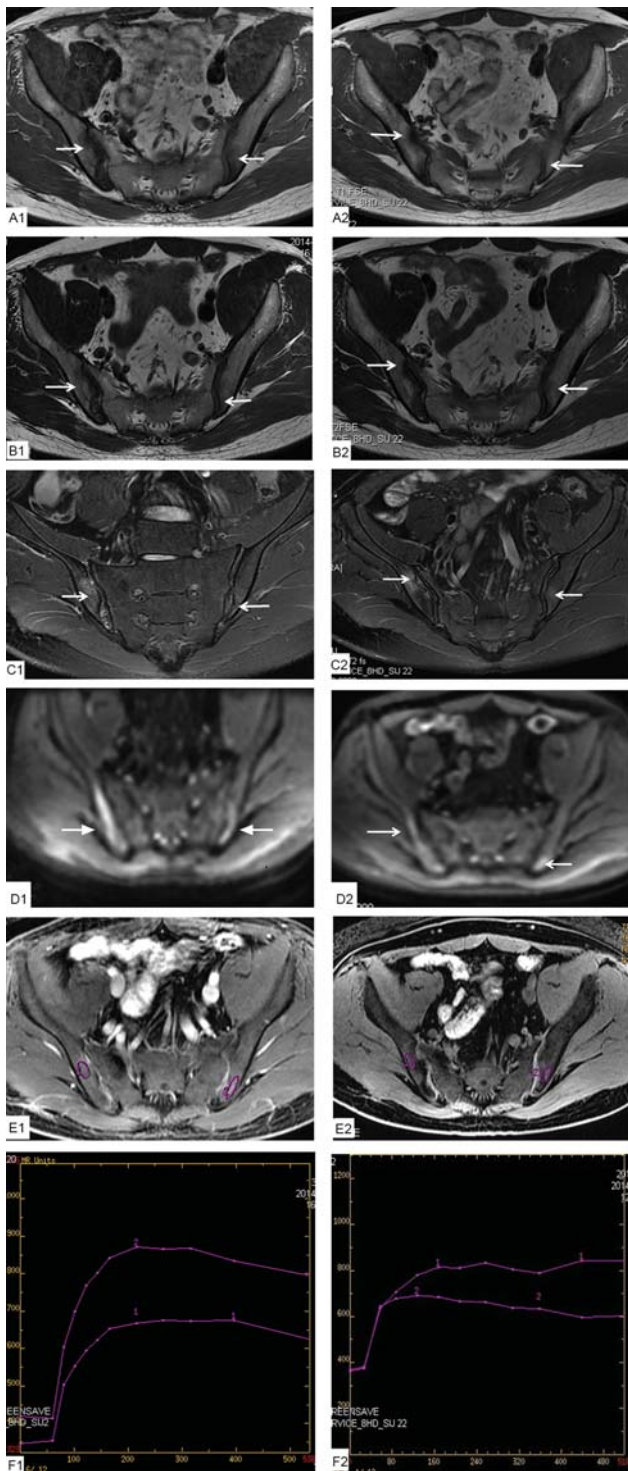


Figure 5. An example for a 24-year-old male patient with AS having chronic lower-back pain over 1 year. The signal characteristics of sacroiliac joint lesions in ankylosing spondylitis is shown from A1toF1 before treatment and the signal changes is shown from A2 to F2 after treatment. Axial T1W-FSE MRI (A1) and Axial T2W-FSE MRI (B1) shows the hypointense lesion in the bilateral ilium (arrow), inhomogeneous high signal on STIR (C1) and significant hyperintense signal on DWI (D1) (arrow). DCE-MRI (E1, F1) shows enhancement Pattern of the lesions and the curve types (red circle), which TIC curve were type II before treatment. After treatment, T1W-FSE MRI (A2) and Axial T2W-FSE MRI (B2) still showed low signal and without marked change (arrow), which high signal intensity was significantly reduced on STIR (C2) and DWI (D2) (arrow). DCE-MRI (E2, F2) shows TIC curve were type II after enhancement, which TTP was extended, and Fenh and Senh were less than before treatment. DCE-MRI =

higher than that of the contrast group because of slight or chronic inflammation.

4.3. DCE changes in early AS after treatment

Dynamic contrast enhanced MRI (DCE-MRI) is a method that visualizes the kinetics of body fluids by rapid injection of a bolus of contrast agent and dynamic imaging of the bolus passage in an organ of interest. Tracer kinetic modeling with DCE-MRI and the quantitative evaluation of the kinetic parameters is a particularly active field of research because the superior spatio-temporal resolution of MRI offers possibilities that are not available to nuclear.^[21]

DCE-MRI is a method that can indirectly reflect the status of blood perfusion and the degree of vascularization through an intravenous injection of water-soluble contrast agent. The changes in hemodynamics take advantage of semiquantitative or qualitative analysis of multiple variable values. The qualitative analysis was performed based on the morphological changes in the TIC curve, and the semiquantitative analysis was performed based on the multivariate analysis of normal tissue or lesion enhancement mode. Therefore, DCE-MRI can not only evaluate the changes in capillary permeability, microcirculation, and blood flow in the lesion area but also directly reflect the blood perfusion rate of the lesion area. In the present study, DCE-MRI is used mainly to observe the degree of blood vessel and the blood flow perfusion in the articular surface bone marrow of the sacroiliac joint in the before- and after-treatment groups, and also to make an objective and real assessment of inflammatory changes and therapeutic effects of AS. The type of TIC curve of the sacroiliac joint was roughly divided into 3 types based on previous studies:^[20]

- (I) as a platform,
- (II) to speed up/slow down, and
- (III) for slow rise/slow down.

In the DCE-MRI follow-up treatment imaging of 48 patients with AS (192 parts), the TIC curve type recorded was as follows: 43.75% (84/192) of type II, 56.25% (108/192) of type III, and type I curve were not seen. The number of type II curve was significantly reduced in the after-treatment group (84 cases) compared with that in the before-treatment group (124 cases). After drawing the TIC curve, the SI_0 , SI_{max} , and TTP were recorded, and the Fenh and Senh values were calculated. The Fenh, Senh, and TTP values before clinical treatment were as follows: Fenh (113.38 ± 44.71) % in ilium and (83.03 ± 20.39) % in sacrum, Senh (60.94 ± 38.56) % min in ilium and (44.91 ± 15.19) % min in sacrum and TTP (129.52 ± 42.66)s in ilium and (123.44 ± 28.50)s in sacrum. Following treatment, Fenh was (75.90 ± 17.97) % in ilium and (73.28 ± 15.67) % in sacrum, Senh was (33.96 ± 11.36) % min in ilium and (31.92 ± 8.15) % min in sacrum, and TTP was (138.67 ± 26.60)s in ilium and (140.19 ± 19.88)s in sacrum. Analyzing the aforementioned data, the Fenh and Senh values after treatment were found to be significantly lower than those of the before-treatment group. The TTP values were longer than those of the before-treatment group (Fig. 5). Significantly statistical differences were observed for

dynamic contrast-enhanced MRI, STIR=short time inversion recovery, TIC= time-signal Intensity Curve, TTP=time to peak, T1W-FSE=T1-weighted fast spin-echo sequence, T2W-FSE=T2-weighted fast spin-echo sequence.

patients between before- and after-treatment groups ($P < .05$). The results exhibited that in the treatment group, the synovial proliferation pannus of the sacroiliac joint lesion area was reduced and absorbed, with vascular permeability recovering and the inflammatory cell infiltration reducing, and the degree of contrast enhancement weakened.

4.4. "Spearman's rho" correlation analysis of ADC, Fenh, and Senh values

In the present study, the "Spearman's rho" correlation analysis was performed between ADC values and Fenh and Senh values in the sacroiliac joint in the treatment group. The correlation coefficient between ADC and Fenh values of the iliac side was $r = 0.744$ and that of the sacral side was $r = 0.702$, which were highly positively correlated. A highly positive correlation existed between ADC and Fenh values of ilium and sacrum, which reflect to some extent that both the ADC and Fenh values rose and fell corresponding to the change in inflammatory activity. From the aforementioned analysis, the present study speculated that the higher the ADC values of the bone marrow zone of the sacroiliac joint, the greater the possibility of the Fenh values of the corresponding site. Similarly, when the degree of Fenh values is higher, the corresponding parts of the ADC values may be higher. The rise and decrease of ADC and Fenh values shift correspondingly with the changes in the inflammatory activity in AS.

Additionally, a significant difference was observed in the ADC and Senh values in the ilium of the sacroiliac joint, and the correlation coefficient were $r = 0.738$, which was highly positive. However, a moderate positive correlation was observed between ADC and Senh values in the sacrum, and the correlation coefficient was $r = 0.547$. A highly positive correlation existed between the ADC and Senh values of ilium, and a moderately positive correlation existed between the ADC and Fenh values of ilium, and it is relevant to the sacroiliac joint special physiological anatomy and the pathological basis of AS. The pannus invasion of ilium side was more easily done compared with the sacrum side so that the vascularization, inflammatory cell infiltration of sacroiliac joints under the surface of the bone, and formation of bone marrow edema appeared earlier, resulting in a higher degree of inflammation, stronger contrast enhancement, and shorter TTP. This is the reason for the difference in performance between the ADC and Senh values of the ilium and sacrum side.

5. Limitations or inadequacies

1. The sample number of the study is relatively small and very strong regionality.
2. All the patients were treated with the combination of Chinese and Western medicine, which the dosage and duration of drugs were not entirely consistent because of difficulty unify the personal specific conditions in all patients, which were its shortages.
3. The diagnostic criteria for AS are human factors, which may lead to false positive results.
4. The follow-up period was relatively short for 6 months, whether long-term treatment is in line with linear regression trend needs further study with longer follow-up times.
5. There was no detailed grouping of gender and not ruled out age the influence of sex and age on bone marrow changes.
6. Semi-quantitative analysis can only show a trend of change, but it is more meaningful without quantitative analysis. We

plan to study the value of quantitative analysis for AS in the future.

6. Conclusion

In conclusion, it is sensitive for conventional MRI sequence to check the high inflammation in patients with AS. For early AS, no obvious bone marrow edema exists, or only a small range of bone marrow edema exists, which is displayed using the conventional MRI scan. The DWI and DCE sequence, which can effectively reflect the AS early treatment condition, and could be applied to access AS inflammation activity changes, reflect the curative effect for patients with early AS, and provide reliable radiological evidence for clinical therapeutic efficacy.

Acknowledgments

Thanks to my teacher's guidance and support. Thanks for the help of my colleagues.

Thanks to clinicians and patients friendly cooperation with us.

Author contributions

Conceptualization: Zhaojuan Shi, Jiankui Han.

Data curation: Jiankui Han, Jian Qin, Yue Zhang.

Formal analysis: Zhaojuan Shi, Jiankui Han, Yue Zhang.

Investigation: Zhaojuan Shi, Jiankui Han, Jian Qin.

Methodology: Zhaojuan Shi, Yue Zhang.

Project administration: Jiankui Han.

Supervision: Jian Qin.

Validation: Zhaojuan Shi.

Visualization: Yue Zhang.

Writing – original draft: Zhaojuan Shi, Jiankui Han.

Writing – review & editing: Jian Qin, Yue Zhang.

References

- [1] Gaspersic N, Sersa I, Jevtic V, et al. Monitoring ankylosing spondylitis therapy by dynamic contrast-enhanced and diffusion-weighted magnetic resonance imaging. *Skeletal Radiol* 2008;37:123–31.
- [2] Ji W, Li J, Lin Y, et al. Report of 12 cases of ankylosing spondylitis patients treated with *Tripterygium wilfordii*. *Clin Rheumatol* 2010;29:1067–72.
- [3] Braun J, Zochling J, Baraliakos X, et al. Efficacy of sulfasalazine in patients with inflammatory back pain due to undifferentiated spondyloarthritis and early ankylosing spondylitis: a multicentre randomised controlled trial. *Ann Rheum Dis* 2006;65:1147–53.
- [4] Jansen JP, Gaugris S, Choy EH, et al. Cost effectiveness of etoricoxib versus celecoxib and non-selective NSAIDs in the treatment of ankylosing spondylitis. *Pharmacoeconomics* 2010;28:323–44.
- [5] Vegvari A, Szabo Z, Szanto S, et al. The genetic background of ankylosing spondylitis. *Joint Bone Spine* 2009;76:623–8.
- [6] Peppmueller PH, Moore TL. Juvenile spondyloarthropathies. *Curr Opin Rheumatol* 2000;12:269–73.
- [7] Razek AA, Tawfik AM, Elsorogy LG, et al. Perfusion CT of head and neck cancer. *Eur J Radiol* 2014;83:537–44.
- [8] Klauser A, Bollow M, Calin A, et al. Workshop report: clinical diagnosis and imaging of sacroiliitis, Innsbruck, Austria, October 9, 2003. *J Rheumatol* 2004;31:2041–7.
- [9] Algin O, Gokalp G, Baran B, et al. Evaluation of sacroiliitis: contrast-enhanced MRI with subtraction technique. *Skeletal Radiol* 2009;38:983–8.
- [10] Althoff CE, Feist E, Burova E, et al. Magnetic resonance imaging of active sacroiliitis: do we really need gadolinium. *Eur J Radiol* 2009;71:232–6.
- [11] Bozgeyik Z, Ozgocmen S, Kocakoc E. Role of diffusion-weighted MRI in the detection of early active sacroiliitis. *AJR Am J Roentgenol* 2008;191:980–6.
- [12] Sourbron SP, Buckley DL. Classic models for dynamic contrast-enhanced MRI. *NMR Biomed* 2013;26:1004–27.

- [13] Zhang M, Zhou L, Huang N, et al. Assessment of active and inactive sacroiliitis in patients with ankylosing spondylitis using quantitative dynamic contrast-enhanced MRI. *J Magn Reson Imaging* 2017;46:71–8.
- [14] HQ. S. Early ankylosing spondylitis sacroiliac joint lesions in MRI [M. S. thesis]. Shandong University. 2007.
- [15] Berman RM, Brown AM, Chang SD, et al. DCE MRI of prostate cancer. *Abdom Radiol (NY)* 2016;41:844–53.
- [16] Razek AA. Diffusion magnetic resonance imaging of chest tumors. *Cancer Imaging* 2012;12:452–63.
- [17] Luna A, Sanchez-Gonzalez J, Caro P. Diffusion-weighted imaging of the chest. *Magn Reson Imaging Clin N Am* 2011;19:69–94.
- [18] Luna A, Martín T, González JS. Diffusion-Weighted Imaging in the Evaluation of Lung, Mediastinum. Springer Berlin Heidelberg: Heart, and Chest Wall; 2012.
- [19] Henzler T, Schmid-Bindert G, Schoenberg SO, et al. Diffusion and perfusion MRI of the lung and mediastinum. *Eur J Radiol* 2010;76:329–36.
- [20] Qin J, Zhao LP, Zhu JZ, et al. The standard values of normal sacroiliac joint on DWI and DCE MRI sequences. *Orthop J Chin* 2014.
- [21] Zikic D, Sourbron S, Feng X, et al. Automatic alignment of renal DCE-MRI image series for improvement of quantitative tracer kinetic studies. *Proc SPIE Int Soc Optic Eng* 1980;167:334–42.